MASS AND HEAT TRANSFER DURING MELTING OF ICE IN SALT SOLUTIONS

A. S. Nevskii and A. I. Malysheva

UDC 536.421.1

This article considers the mechanism by which ice melts in salt solutions. Experimental data were used to determined the coefficients of mass transfer from dissolved NaCl to the melting surface during natural convection and forced movement and when air was bubbled through the solution.

The melting of any substance when its melting point is reduced by contact between the liquid and a solid is of great interest. Special cases of this phenomenon include the melting of ice in salt solutions and the melting of iron in iron–carbon melts. These processes are defined by two equations: the mass-transfer equation and the heat-transfer equation. Although both phenomena belong to the same class, they differ from one another. When ice melts, substances dissolved in the water do not form a solid solution with the ice, while carbon dissolved in molten iron is capable of forming a solid solution with the latter. This introduces some difference into the course of the processes. We will consider only the first case in the present article.

We construct the salt-balance equation at the melting surface:

$$\beta (C_{\mathrm{p}} - C_s) = w_{\mathrm{m}} C_s \rho. \tag{1}$$

The left-hand side of the equation represents the amount of salt reaching the melting surface by diffusion. The right-hand side represents the amount of salt necessary to maintain a concentration C_s at the boundary between the liquid phase and the melting surface. Similarly, we write the heat-transfer equation:

$$\alpha (t_{\mathrm{p}} - t_s) = w_{\mathrm{m}} \rho q_{\mathrm{m}} \tag{2}$$

From Eqs. (1) and (2) we obtain

$$t_{\mathrm{p}} - t_s = t_0 \left(\frac{C_{\mathrm{p}}}{C_s} - 1 \right),$$

or

$$\frac{t_{\mathrm{p}} - t_s}{C_{\mathrm{p}} - C_s} = \frac{t_0}{C_s}, \tag{3}$$

where

$$t_0 = \frac{\beta q_{\mathrm{m}}}{\alpha}. \tag{4}$$

If t_0 is known, Equation (3) contains two unknowns: the salt concentration C_s and the temperature t_s at the boundary with the melting surface. We will assume that these quantities are associated with the liquidus curve for the equilibrium state of the ice–salt solution system. Equation (3), together with the liquidus curve, then enables us to determine the values of these quantities.

We can give graphic interpretation of the solution of this equation. We mark off points A and B, indicating the solution temperature (A) and the unknown melting-surface temperature (B), on the ordinate of the equilibrium phase diagram for the system (Fig. 1), which corresponds to the salt concentration in the

---

Scientific-Research Institute of Metallurgical Heat Engineering, Sverdlovsk. Translated from Inzhenerno-Fizicheskii Zhurnal, Vol. 19, No. 4, pp. 652-658, October, 1970. Original article submitted December 11, 1969.

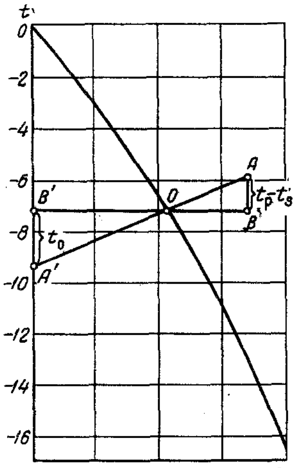

Fig. 1

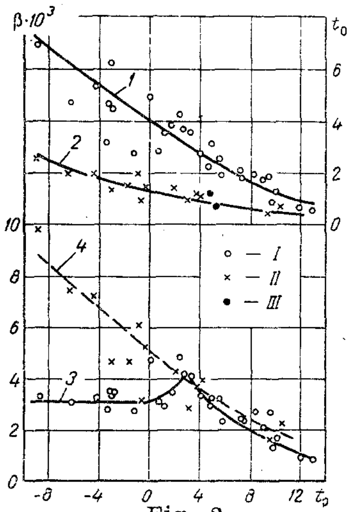

Fig. 2

Fig. 1. Diagram for a determination of the temperature difference between solution and melting surface. t) temperature, °C; C_p) NaCl concentration, %.

Fig. 2. Dependence of t_0 (curves 1 and 2) and β, kg/(m^2 · sec), (curves 3 and 4) on solution temperature under natural-convection conditions (1 and 3) and during forced flow (2 and 4). I) Observations made with natural convection; II) observations for forced flow; III) observations made under impact of jet.

solution C_p. The point O where a line passing through point B and parallel to the abscissa intersects the liquidus defines the salt concentration in the solution at the boundary with the melting surface C_s. We continue lines AO and BO to their intersection with the ordinate, which corresponds to a salt concentration of zero. This yields points A' and B'. From the similarity of the triangles AOB and A'OB', we have

$$\frac{AB}{OB} = \frac{A'B'}{OB'} . \tag{5}$$

It follows from our construction that

$$\left.\begin{aligned} AB &= t_p - t_s , \\ OB &= C_p - C_s , \\ OB' &= C_s , \end{aligned}\right\} \tag{6}$$

i.e.,

$$\frac{t_p - t_s}{C_p - C_s} = \frac{A'B'}{C_s} . \tag{7}$$

It can be seen from a comparison of Eqs. (7) and (3) that the segment A'B' equals the quantity t_0.

This construction gives us a graphic interpretation of the process and facilitates solution of Eq. (3).

The melting rate is determined by the coefficient of heat transfer from the solution to the melting surface and by the temperature difference in the solution far from this surface and at the boundary with it. The first quantity is governed by hydrodynamic factors, while the latter is determined by the solution temperature and t_0. If the heat-transfer constant and t_0 are known, the melting rate can be calculated.

The above relationships can be utilized for experimental determination of the coefficients of mass transfer. For this purpose, it is necessary to determine the melting point of the solid experimentally and to calculate the heat-transfer coefficient from the melting rate. We find t_0 by using the liquidus curve and calculate the mass-transfer coefficients β from Eq. (4).

TABLE 1. Principal Experimental Data

NaCl concentration in solution C_p, %	Solution temperature t_p, °C	Velocity w, m/sec	Melting point t_s, °C	NaCl concentration at melting surface C_s, %	Heat-transfer coefficient α, W/m^2·deg	t_0, deg	Mass-transfer coefficient $\beta \cdot 10^3$ kg/m^2·sec
17,3	4,1	0	—3,0	4,85	395	2,77	3,342
17,0	5,6	0	—2,5	4,1	415	2,57	3,255
16,7	8,4	0	—1,65	2,75	455	1,98	2,733
17,1	3,3	0	—3,6	5,8	375	3,54	4,078
17,0	5,6	0	—2,5	4,1	417	2,57	3,270
16,5	7,4	0	—1,65	2,75	440	1,81	2,410
17,4	2,7	0	—3,9	6,25	370	3,70	4,210
17,4	9,6	0	—1,5	2,5	480	1,86	2,707
16,6	12,0	0	—0,45	0,8	505	0,63	0,958
11,9	5,0	0	—2,2	3,6	350	3,12	3,324
11,7	7,3	0	—1,35	2,3	380	2,12	2,434
11,6	9,1	0	—1,0	1,7	417	1,73	2,183
12,2	—3,0	0	—5,6	8,6	176	6,21	3,398
12,4	1,8	0	—3,3	5,35	295	3,87	3,497
12,2	1,2	0	—3,3	5,35	276	3,52	2,972
13,5	10,1	0	—0,8	1,4	450	1,26	1,712
23,5	—3,4	0	—7,2	10,7	285	3,18	2,845
22,7	—1,2	0	—5,8	8,9	320	2,77	2,756
22,2	0,8	0	—4,8	7,5	355	2,86	3,138
23,1	4,8	0	—3,15	5,15	427	2,28	2,983
22,6	9,8	0	—1,0	1,7	505	0,88	1,339
22,1	13,0	0	—0,45	0,8	550	0,51	0,835
22,6	—8,8	0	—11,8	15,8	150	6,97	3,388
22,6	—6,2	0	—9,5	13,3	205	4,72	3,087
17,3	—2,9	0	—6,4	9,7	250	4,47	3,492
16,9	0,1	0	—5,25	8,1	310	4,92	4,732
17,5	—3,2	0	—6,7	10,0	243	4,67	3,551
17,2	2,5	0	—4,2	6,7	365	4,28	4,824
16,8	5,8	0	—2,0	3,3	410	1,91	2,376
16,3	—4,2	0	—7,1	10,55	200	5,32	3,344
20,8	—1,65	0,066	—4,5	7,1	1010	1,48	4,605
20,8	3,15	0,068	—1,9	3,2	1030	0,92	2,870
21,2	—6,35	0,080	—8,0	11,65	1170	2,01	7,440
21,2	—3,15	0,081	—5,2	8,1	1175	1,27	4,620
21,2	—0,65	0,081	—3,3	5,3	1175	0,88	3,179
20,0	10,45	0,083	—0,6	1,05	1210	0,61	2,230
21,0	—8,95	0,082	—10,2	14,1	1200	2,55	9,824
21,0	—4,4	0,081	—6,6	9,9	1175	1,96	7,216
21,0	—0,35	0,083	—3,8	6,1	1210	1,41	5,252
21,0	4,15	0,083	—1,9	3,15	1210	1,07	3,925
21,0	9,45	0,086	—0,5	0,85	1250	0,42	1,580
19,3	—0,9	0,064	—4,4	7,0	990	1,99	6,085
19,3	1,95	0,066	—2,7	4,4	1015	1,37	4,253
19,3	3,75	0,068	—2,0	3,3	1030	1,19	3,711
19,3*	5,36	—	—1,1	1,9	—	0,70	—
19,3*	4,95	—	—1,8	3,0	—	1,24	—

---

* Melting under impact of jet.

Such calculations have been made on the basis of experiments on the melting rate of ice cylinders in NaCl solutions under natural-convection conditions and with forced motion of the solution, which flowed by the cylinder at rates of up to 0.086 m/sec [1]. Using thermocouples frozen into the cylinders, we determined the melting point t_s. The cylinders were 62-72 mm in diameter and 66-85 mm long. Table 1 gives the principal data obtained in these experiments.

The boundary concentrations C_s were determined from the temperature t_s and the equilibrium curve for the NaCl solution–ice system (Fig. 1); t_0 was determined from Eq. (3) and the mass-transfer coefficient from Eq. (4), where q_m was calculated from the formula

$$q_m = (79.6 + 0.5\,t_s)\,4.187\ \text{kJ/kg}. \qquad (8)$$

Figure 2 shows t_0 as a function of melt temperature for natural-convection conditions (curve 1) and forced flow (2). There was a decrease in t_0 as the melt temperature rose in both cases. We used the results of observations made with different NaCl concentrations in the solution (from 11.6 to 23.5% for natural

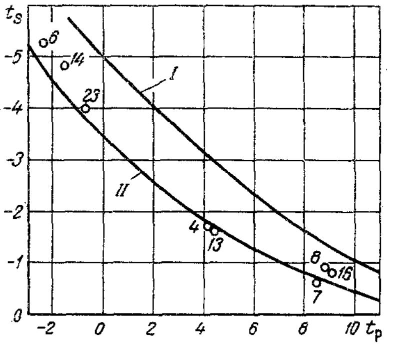

Fig. 3

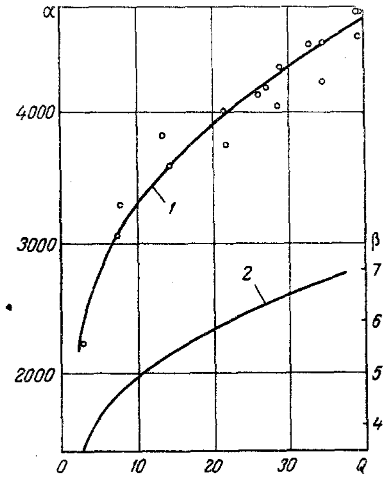

Fig. 4

Fig. 3. Melting point t_s as a function of solution temperature t_p in experiments with air bubbled through bath.

Fig. 4. Heat-transfer coefficient α, W/m^2·deg, (1) and mass-transfer coefficient $\beta \cdot 10^{-3}$, kg/m^2·sec, (2) during melting of ice cylinders with air bubbled through bath at t_p = 10°C and C_p = 20% as a function of air delivery rate Q, liters/min.

convection and from 19.3 to 21.2% for forced flow). No relationship was found between t_0 and the concentration. The points designated are for melting of ice under the impact of a jet of solution with a concentration of 19.3%.

Figure 2 also shows the mass-transfer coefficient β as a function of solution temperature (curves 3 and 4).

We analyzed the possible errors in determining β. The maximum possible error in the solution temperature was assumed to be 0.1°C, while that in the melting point was assumed to be 0.2°C. The maximum error in determining β for $C_p \simeq 22\%$ was found to reach 17-18% at moderate temperatures (between −4 and +4°C). It increased at lower and higher temperatures and was especially large when the solution temperature was raised to 10-12°C. The error was also larger for smaller NaCl concentrations.

It can be seen from Fig. 2 that, with forced flow of the solution, the coefficient β decreased as the solution temperature was raised, obviously as a result of the increase in the mass of the melted water screening the solid from penetration of salt to its surface.

The relationship between β and t_p for natural convection in the solution-temperature region 3-12°C was almost identical to the graph for forced convection. At lower temperatures, β decreased as the temperature was reduced and subsequently became stable. This trend for the natural-convection graph is apparently explained by the low mobility of the liquid at low temperatures, a phenomenon actually observed during the experiments. The peak in the curve for β at 3° was evidently due to the known anomaly in the density of water at low temperatures, which causes an increase in solution turbulence near the melting of surface.

It was established in these experiments that the melting point was raised when the rate at which the solution flowed by the ice cylinder was increased to 0.065-0.086 m/sec. However, this increase did not exceed 1.5°C and was less in most cases, which impeded the determination of the dependence of the temperature on flow speed. Our investigations enable us to hypothesize that there is no change in melting point when the solution flow speed is increased above 0.065-0.08 m/sec. Unfortunately, the technical capabilities of the apparatus did not permit us to increase the flow speed to above 0.086 m/sec.

In order to verify the above hypothesis, we conducted two experiments involving a determination of the melting point of ice under the impact of a solution jet. The melting point in this case was found to be the same as for a flow speed of 0.08 m/sec [1].

In order to further clarify this problem, we determined the melting point of ice and the heat-transfer coefficients during melting with artificial solution turbulence produced by bubbling air through the solution; the experiments involved the melting of ice cylinders 64 mm in diameter and 70-80 mm long in a rectangular bath with an area of 225 × 220 mm^2 and a depth of 235 mm. The cylinders were immersed in the solution in the center of the bath so that their upper ends were 55 mm below the solution level. Air was forced through 50 holes 1 mm in diameter located in the bottom of the bath beneath the ice cylinder, around the circumference of a circle 65 mm in diameter. The bubbles rose, passing around the bottom and sides of the cylinder and vigorously agitating the solution near the ice surface.

Curves I and II (Fig. 3) show the melting point t_s as a function of solution temperature [1] for natural convection (I) and for forced solution flow with $w \sim 0.08$ m/sec (II). This graph also shows the melting points obtained with air bubbled through the bath (the figures beside the points indicate the amount of air bubbled through in liters per minute). It can be seen from Fig. 3 that the melting point and hence t_0 were virtually the same when air was bubbled through the bath at a rate of no less than 4 liters/min as when the solution flowed around the cylinders at a rate of 0.08 m/sec and were independent of the bubbled-air delivery rate.

Figure 4 shows the heat-transfer coefficient as a function of the air delivery rate at $t_p = 10°\text{C}$ and $C_p = 20\%$. It can be seen from Fig. 4 that bubbling greatly increased the value of α. As was pointed out above, t_0 was independent of the bubbling rate. In accordance with Fig. 2, t_0 can therefore be assumed to be 0.5° for the experiments shown in Fig. 4. Using (4), we find

$$\beta = 0.5\, q_m^{-1}\alpha \approx 0.0015 \cdot 10^{-3}\, \alpha \text{ kg/m}^2 \cdot \text{sec}. \tag{9}$$

Figure 4 also shows the curve for the coefficient β.

The melting point is thus minimal and t_0 is high with a low degree of liquid turbulence. When the turbulence is slightly increased, the melting point rises slightly and t_0 decreases, which indicates that the mass-transfer coefficient rises more slowly than the heat-transfer coefficient. However, the melting point and hence t_0 very quickly become independent of the turbulence intensity, i.e., the two coefficients exhibit a proportional rise.

NOTATION

C_p	is the NaCl concentration in solution, kg/kg or %;
C_s	is the same, at melting surface;
t_p	is the solution temperature, °C;
t_s	is the same, at melting surface;
w	is the velocity of solution, m/sec;
q_m	is the latent heat of melting, J/kg;
α	is the heat-transfer coefficient, $\text{W}/(\text{m}^2 \cdot \text{deg})$;
β	is the mass-transfer coefficient, $\text{kg}/(\text{m}^2 \cdot \text{sec})$;
w	is the melting rate, m/sec.

LITERATURE CITED

1. A. S. Nevskii and A. I. Malysheva, in: Heat and Mass Transfer [in Russian], (A. V. Lykov and B. M. Smol'skii, editors), Vol. 2, Nauka i Tekhnika, Minsk (1968).